ELSEVIER

Brain Research 665 (1994) 18–32

BRAIN RESEARCH

Research report

Electrophysiology and morphology of neurons in rat perirhinal cortex

John M. Beggs, Edward W. Kairiss *

Department of Psychology, Yale University, PO Box 208205, New Haven, CT 06520-8205, USA

Accepted 23 August 1994

Abstract

The intrinsic membrane properties of perirhinal cortical neurons were studied by intracellular recording in in vitro rat brain slices. Gross morphology was also examined through injection of the fluorescent dye carboxyfluorescein. The cells encountered displayed a diversity of electrophysiological properties, and were similar to cells reported in other neocortical areas with regard to spiking patterns, afterpotentials, and morphology. However, very few (4%) intrinsically bursting neurons were encountered. Two pyramidal cells with thick apical dendrites were filled, and both fired doublets of action potentials for their first suprathreshold events. Of the filled pyramidal cells with thin apical dendrites, most (9/11) fired single action potentials for their first suprathreshold events. A variety of classification schemes were used to group the data, and several schemes were found to be equally successful. According to one of the schemes, cells recorded with carboxyfluorescein filled electrodes had significantly greater action potential widths at half-amplitude and more depolarized resting potentials than cells recorded without this dye.

Keywords: Perirhinal cortex; Intracellular recording, in vitro; Intrinsic property

1. Introduction

To understand the organization of a brain region, it is often necessary first to classify its various cell types. Recently, cell classification combining morphology and electrophysiology has been applied to several regions of neocortex [3,9,11,14,15,16,17,26]. A summary of these findings [5] indicates that neocortical neurons can be grouped into three general classes: RS, IB, and FS cells.

Regular-spiking (RS) cells are the most common type found in intracellular recording studies, and have either pyramidal or spiny stellate morphology [15,16,17]. They show spike-frequency adaptation when injected with a depolarizing current step [4].

Intrinsically bursting (IB) cells are the next most common type encountered with sharp electrodes. IB cells are also pyramidal with spines, although their apical dendrites are thicker than those of RS cells [15,16,17]. The distinguishing feature of IB cells is a 'burst' of action potentials fired on the crest of a depolarizing wave in response to depolarizing current injection [4].

Finally, fast-spiking (FS) cells are rarely recorded through intracellular electrodes, although correlative morphology indicates that they are numerous and can be found in almost every cortical layer [17]. Dye injection has shown them to be aspiny, with stellate morphologies, while immunohistochemistry has shown them to be GABAergic, suggesting that they are inhibitory [17]. In response to depolarizing current steps, FS cells exhibit tonic firing of action potentials without accommodation.

Although this scheme has described the cells encountered in most cortical areas examined so far, there is a need to see if it applies to the rest of cortex as well. Foehring et al., for example, did not find any IB cells in human association cortex [9]. Is this merely a species difference, or is it a property of association cortex? All but one of the rodent papers published to date have focused on primary sensory or motor cortex. It would be of particular interest to know if there is a reduced population of IB cells in rodent association cortex, a neglected area.

Rat perirhinal cortex has several features that qualify it as an association cortex. Defined to occupy por-

* Corresponding author. Fax: (1) (203) 432-7172; E-mail: kairiss@milner.psych.yale.edu

0006-8993/94/$07.00 © 1994 Elsevier Science B.V. All rights reserved
SSDI 0006-8993(94)01050-1

tions of cytoarchitectonic areas 35 and 13, rostral perirhinal cortex begins where the claustrum ends and continues caudally along the dorsal and ventral banks of the rhinal sulcus [25]. Perirhinal cortex receives inputs from a variety of other higher order cortical areas, including anterior cingulate, temporal, parietal, and lateral occipital cortices [7].

Several studies also suggest that perirhinal cortex plays a role in certain forms of memory in rat [2,28] and monkey [19,22,32,36]. Further, it is known that the perirhinal cortex has extensive reciprocal connections with the amygdala [13,18,24], a structure necessary for the acquisition of fear-conditioning [6]. Recent in vitro work has shown that perirhinal cortex and the amygdala can be contained together in a slice, along with functional connectivity between them [12]. Thus, a cell classification study of perirhinal neurons could lay the foundation for later inquiries into synaptic plasticity between these two areas.

Another question about cell classification concerns the scheme itself: could several alternative classification schemes be developed to successfully group cell types? Past studies have grouped cells on the basis of several identifiers: spike-frequency adaptation, action potential bursts, action potential width, and types of afterpotentials, for example [4,16,17]. If these identifiers are distributed, do they form distinct clusters, or are they uncorrelated and spread over a broad range? In the former case, RS, IB, and FS cells would be prototypes lying at the centers of these clusters, and would probably represent a natural grouping. In the latter case, these labels would not identify cell types, but would merely label the domains of one of the possible grouping schemes. A closer examination of other classification schemes has not been done in previous studies.

The present study was motivated by three goals: first, to examine the electrophysiological and morphological properties of the cells encountered in the unexplored area of perirhinal cortex. Second, to lay the foundation for further studies of perirhinal cortex that may use information about cell classes. Third, to examine several possible classification schemes to see if more than one scheme could be used with success in grouping cells.

2. Materials and methods

2.1. Slicing procedure

Sixty male Sprague–Dawley rats were used, weighing between 75–300 g, with ages between 21 and 40 days. The rats were deeply anesthetized with halothane and decapitated. For dissection, the skin above the skull was cut back, and the cranium was opened along the fissures to expose the brain. After taking care to retract the dura, the brain was immediately removed and transferred to cold (3°C) artificial cerebrospinal fluid (ACSF) which was saturated with 95% O_2/5% CO_2 (carbogen). While in ACSF, a block of cortex containing the rhinal sulcus (bregma −1.80 to −4.80) was cut away. This was glued with cyanoacrylate onto a petri dish mounted in a tissue slicer (Vibratome series 1000). While bathing in 3°C ACSF, 4–5 coronal slices were cut, each to a thickness of 400 μm. Slices were then transferred to a beaker of ACSF saturated with carbogen and allowed to equilibrate for at least one hour before recording.

Perirhinal slices prepared in this way were viable for over 12 h but displayed little spontaneous activity. In these respects, perirhinal slices were similar to slices that this laboratory has worked with from hippocampus and visual cortex.

2.2. ACSF composition

The ACSF contained (in mM): NaCl 124, KCl 2, $NaH_2PO_4 \cdot H_2O$ 1.25, $NaHCO_3$ 26, D-glucose 10, $MgSO_4 \cdot 7H_2O$ 2, $CaCl_2 2H_2O$ 2.

2.3. Slice chamber

Slices were placed in an interface chamber (Fine Science Tools) and supported on a nylon mesh platform covered with lens paper. ACSF saturated with carbogen was passed below the slices, while a warmed and humidified atmosphere of carbogen was passed above. Temperature was thermostatically maintained at 32 ± 0.9°C (mean ± S.D.).

2.4. Electrophysiological techniques

Electrodes were pulled to resistances of 60–120 MΩ (Brown-Flaming puller) using 1 mm thin-walled capillaries (WP Instruments) filled with 4 M KAc. To measure current–voltage relationships, a series of current steps (−1.0 to 1.5 nA, increments of 0.1 nA, 160 ms) was injected through the recording electrode. Current commands were issued via computer control (Stoelting Laboratory Controller) and sent to a current clamp amplifier (Axoclamp-2A). Data were sampled at 20 kHz (Cambridge Electronic Design VClamp program), and the electrode headstage was continually monitored for adequate capacitance compensation. Recordings were usually performed at resting potential in bridge mode. In cases where negative holding current was applied, it did not exceed −0.3 nA, and recordings were made in discontinuous current-clamp mode to avoid nonliniarities in electrode resistance.

2.5. Cell staining

For intracellular labeling, electrode tips were filled with 5% 5-(and 6-)carboxyfluorescein (Molecular Probes) in 0.1 M KAc and backfilled with 4 M KAc, a procedure which usually increased resistances by 50%. Dye was injected with hyperpolarizing current pulses (100 ms, −0.1 to −1.0 nA) in a 50% duty cycle for at least 5 min. Because 5-(and-6)-carboxyfluorescein is not a fixable tracer, slices were removed from the recording chamber for visualization immediately after dye injection. They were cleared in glycerol for 5 min and then mounted on slides and viewed under ultraviolet light using an Olympus T041 microscope.

2.6. Location of cells

Electrode placement was done under visual guidance through a 40× dissection microscope (Olympus SZ40). While looking through this objective, it was possible to view the full thickness of the cortical area in question from pia to white matter. The penetration point of the recording electrode could always be clearly identified, and from

this, the location of the cell was estimated to be in either the upper, middle, or lower third of the cortex.

2.7. Data collection and statistics

The analog signals were digitally converted by a CE Design 1401 A-D converter and recorded to disk using the VClamp program running on a Sun 386i computer. The stored waveforms were measured for a variety of features (given below) using a program written by the authors in PV-Wave language and run on a Sun workstation. Statistical analysis of the measured quantities was accomplished with a SAS package run on a personal computer (see Fig. 1).

List of the variables used in classification:

AB THRES (absolute threshold) = the voltage where the angle of the tangent line triples within 3 ms, and this is found to agree with visual inspection of where the action potential begins

AMP (amplitude) = V(A) − V(AB THRES)

HW (half width) = action potential width at half-amplitude

REL THRES (relative threshold) = V(VM) − V(AB THRES)

BASELINE = V(D) − V(VM) – this is taken at a point after the afterpotentials, yet before the end of the current step

AHP AMP (afterhyperpolarization amplitude) = V(B) − V(AB THRES)

ADP AMP (afterdepolarization amplitude) = V(C) − V(AB THRES)

AHP LAT (afterhyperpolarization latency) = t(B) − t(A)

ADP LAT (afterdepolarization latency) = t(C) − t(A) – afterpotential events that occurred within 20 ms of the action potential were classified as fADP or fAHP. Afterpotentials later than this were classified as sADP or sAHP

RISE = the slope of the action potential taken from leading edge at half-amplitude to the peak

FALL = the slope of the action potential taken from the peak to the trailing edge at half-amplitude

MX RISE = the maximum positive value of dV/dt obtained

MX FALL = the maximum negative value of dV/dt obtained

dV/dt RATIO = −1 × MX RISE/MX FALL)

RIN = the slope of the line fitted by least squares to the linear portion of the plot of membrane voltage vs. injected current – membrane voltage was measured 120 ms after the start of the 160 ms current pulse

TAU = the slope of the line fitted by least squares to the plot of ln(voltage) vs. time – the line was fitted to the discharge portion of the voltage trace that occurred after the −0.2 nA step was turned off

IHOLD = the amount of holding current applied through the electrode during the recordings

INT1, INT2, INT3 = the first, second, and third interspike intervals, respectively

ISI SLOPE = the difference between the first two interspike intervals, when they both exist in a single trace

FI SLOPE = the slope of the line fitted by least squares to the first four points of the plot of frequency (first interval) vs. injected current

SAG (%) = $100 \times [(V_{peak} - V_{steady\ state})/V_{peak}]$, where V_{peak} is the most hyperpolarized voltage reached during the pulse, and $V_{steady\ state}$ is taken just before the end of the hyperpolarizing current pulse (Stafstrom et al. [31])

UNDERSH (%) = $100 \times (V_{peak}/V_{steady\ state})$, where V_{peak} is the most hyperpolarized voltage reached after a depolarizing pulse has been turned off, and $V_{steady\ state}$ is taken just before the pulse is turned off.

3. Results

A total of 93 cells were recorded from cytoarchitectonic areas 35 and 13, including both the dorsal and ventral banks of the rhinal sulcus. Of these, 14 cells were recorded with carboxyfluorescein in the electrode (group dye-filled; DF), and 79 were recorded without dye (group dye-unfilled; DU). To investigate possible effects of carboxyfluorescein, separate analyses were performed on these two groups.

3.1. Selection criteria

To establish reasonable selection criteria, two independent methods were tried. First, only cells with resting membrane potentials hyperpolarized with respect to −50 mV (one of the criteria used by other researchers in cortex [9]) and with input resistances greater than 20 MΩ were accepted. These criteria yielded group sizes of 71 (DU) and 10 (DF). The resulting distribution of these variables is given in Table 1 under 'standard criteria'. A second approach was used independently to avoid applying selection criteria frequently used by others in cortical areas. Here, distributions of resting membrane potential (VM), input resistance (RIN), action potential amplitude (AMP), and action potential width at half-amplitude (HW) were examined for 'outliers' according to a Tukey box plot [35] (where an outlier is over three interquartile ranges beyond the mean). The outliers were then excluded, and analysis was conducted on the remaining cells. When this was done, 70 DU cells and 10 DF cells remained. The DF cells remaining had their variables distributed over the ranges indicated in Table 1 under 'outlier criteria'. A total of 35 character-

Table 1
Ranges resulting from selection criteria

Variable	Standard		Outlier	
	DU	DF	DU	DF
Number	(n = 71)	(n = 10)	(n = 70)	(n = 10)
VM (mV)	−50.5 ... 97.4	−51.0 ... −77.4	−44.7 ... −90.8	−37.6 ... 73.1
RIN (MΩ)	20.2 ... 94.2	25.3 ... 80.0	13.1 ... 61.9	25.3 ... 36.3
AMP (mV)	33.5 ... 68.4	42.5 ... 53.1	26.6 ... 68.4	42.5 ... 53.1
HW (ms)	0.65 ... 4.6	0.9 ... 3.1	0.6 ... 2.0	0.9 ... 3.1

Ranges of selected variables under standard and outlier selection criteria. Standard selection excluded all cells with VM < −50 mV and RIN < 20 MΩ. Outlier selection criteria excluded all cells that were determined to be 'outliers' when distributions were placed on a Tukey box plot (Tukey, 1977).

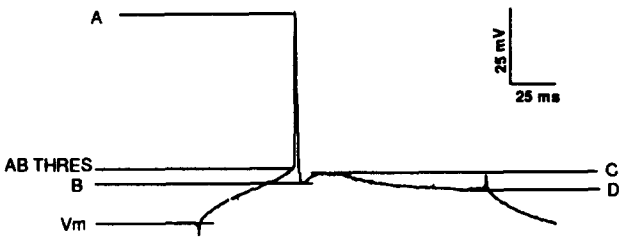

Fig. 1. Markers for variables measured. Cartoon represents voltage response to depolarizing current step. Line segments at VM, A, B, C and D are drawn tangent to the curve where $dV/dt = 0$. Variables described in section 2 are defined in terms of these markers.

istics were measured for each cell (see subsection 2.7).

After this initial screening, it was still necessary to test if the distributions were influenced by the quality of the microelectrode impalement. Ideally, variations in VM, AMP, and HW would reflect natural variations in the population of cells. The possibility existed, however, that low VM, for example, might be caused by poor microelectrode impalement as reflected by low RIN. To examine such relationships, Pearson correlation coefficients were obtained in each group (DU, DF) for the four variables VM, RIN, AMP, and HW. For both DU and DF cells under both 'standard' and 'outlier' selection criteria, none of the variables were significantly correlated to VM ($P > 0.05$). These results indicate that the quality of impalement, as given by RIN, did not contribute to variations in these measurements.

3.2. Dye effects

To examine the effects of carboxyfluorescein, one-way analyses of variance (ANOVAs) were performed on VM, RIN, AMP, and HW with respect to the presence of the dye in the electrode. No significant differences were found among these variables with respect to dye in the cells screened by the outlier selection method. In the cells screened by the standard method, it was found that VM and HW were significantly different ($P < 0.05$ level), suggesting that carboxyfluorescein contributed to depolarized VM and broadened HW.

3.3. Cell classes

Each cell was measured for 26 continuous variables which described various aspects of its membrane responses to injected current steps (variables are described in the list following Fig. 1). To search for natural divisions among the data set, distributions of these variables were plotted in histograms, where the optimal bin width was chosen by the SAS chart procedure according to the methods of Terrell and Scott [33]. Briefly, bin widths were chosen to minimize the integrated means-squared error between the smoothed distribution and the actual data. When inspected, most of these distributions appeared unimodal, and there were no obvious points where they could be divided.

Table 2
Partitions of continuous distributions

variable	AMP < 55 mV	INT 1 < 7.5 ms	INT 2 < 42 ms	TAU < 20 ms	SAG < 4%
Below partition	$n = 41$	$n = 31$	$n = 57$	$n = 42$	$n = 54$
Above partition	$n = 23$	$n = 33$	$n = 7$	$n = 22$	$n = 10$
RIN (MΩ)				**	
AMP (mV)			**	**	
HW (ms)	*				
TAU (ms)		**			
IHOLD (nA)	**	*		**	
ISI SLOPE (ms/interval)		**	**	**	
FI SLOPE (Hz/nA)			**		
INT 1 (ms)			*	*	
AB THRES (mV)	**	**			
RL THRES (mV)	*				
BASELINE (mV)	**	*			
RISE (V/s)	**				
FALL (V/s)			*		
MX RISE (V/s)	**		**		
MX FALL (V/s)	**		*		
UNDERSH (%)	*				
fAHP AMP (mV)	*				
significant differences	10	5	7	5	0

Statistically significant differences resulting from partitions of continuous variables of DU cells. Cells in this table were screened by standard and outlier cutoff methods, resulting in a sample size of 64. Each division (except for INT 1) was made at a notch in the distribution that seemed to naturally divide it into two groups. All distributions of continuous variables showing notches were divided this way. Although the INT 1 distribution did not show a notch, it was arbitrarily divided as a test. The two groups resulting from each division were then tested for significant differences using a one-way ANOVA. Variables that were significantly different are indicated by asterisks (* $P < 0.05$, ** $P < 0.01$).

Table 3
Partitions by categorical variables

	AP PAIR	fAHP	fADP	sAHP	sADP
Present	$n = 15$	$n = 56$	$n = 26$	$n = 37$	$n = 4$
Absent	$n = 49$	$n = 8$	$n = 38$	$n = 27$	$n = 60$
HW (ms)	**				**
ISI SLOPE (ms/interval)					
FI SLOPE (Hz/nA)		*		**	
INT 1 (ms)	*			*	
INT 2 (ms)				*	
INT 3 (ms)				*	
BASELINE (mV)				**	
RISE (V/s)	*				
MX RISE (V/s)				*	
MX FALL (V/s)	**				
fAHP LAT (ms)	**			*	
sAHP LAT (ms)					**
fAHP AMP (mV)	*			**	*
fADP AMP (mV)				*	
AP PAIR			*		
significant differences	6	1	1	9	3

Statistically significant differences resulting from partition by categorical variables of DU cells. Cells in this table were screened by standard and outlier selection criteria, resulting in a sample size of 64. Cells possessing the categorical variable were separated from those not possessing it. The two groups thus formed were tested for significant differences using one-way ANOVAs. Variables that were significantly different are indicated by asterisks (* $P < 0.05$, ** $P < 0.01$).

Table 4
Singlet and doublet variables

Variable	Singlet	Doublet	Significance
n	56	14	
VM (mV)	69.6 ± 10.6	68.3 ± 9.9	
RIN (MΩ)	34.8 ± 10.5	35.6 ± 7.7	
AMP (mV)	49.5 ± 9.1	55.6 ± 5.8	*
HW (ms)	1.3 ± 0.3	1.0 ± 0.2	*
TAU (ms)	20.6 ± 7.3	16.9 ± 5.8	
IH (nA)	−0.1 ± 0.2	−0.2 ± 0.2	
ISI SLOPE (ms/interv)	5.7 ± 6.0	3.1 ± 3.2	
FI SLOPE (Hz/nA)	89.1 ± 86.6	77.8 ± 77.0	
INT 1 (ms)	10.3 ± 7.1	5.9 ± 1.2	**
INT 2 (ms)	20.9 ± 17.1	21.4 ± 21.4	
INT 3 (ms)	27.4 ± 23.5	44.9 ± 25.8	
AB THRES (mV)	34.5 ± 12.6	37.8 ± 11.0	
RL THRES (mV)	35.2 ± 12.0	30.6 ± 11.8	
BASELINE (mV)	44.0 ± 13.4	47.6 ± 13.0	
RISE (V/s)	39.3 ± 10.6	47.6 ± 8.5	**
FALL (V/s)	40.6 ± 17.6	44.1 ± 47.9	
MX RISE (V/s)	84.5 ± 69.6	117.2 ± 76.7	
MX FALL (V/s)	46.6 ± 16.8	72.6 ± 24.0	**
dV/dt	1.9 ± 1.3	1.6 ± 0.8	
UNDERSH (%)	36.8 ± 17.3	14.5 ± 16.9	
SAG (%)	3.0 ± 6.2	2.4 ± 4.9	
fAHP LAT (ms)	4.3 ± 2.7	2.4 ± 0.8	*
fADP LAT (ms)	10.7 ± 6.5	5.6 ± 1.1	
sAHP LAT (ms)	46.0 ± 25.0	50.0 ± 30.0	
sADP LAT (ms)	31.8 ± 9.4	0.0 ± 0.0	
fAHP AMP (mV)	0.9 ± 8.1	10.3 ± 6.1	**
fADP AMP (mV)	1.8 ± 8.8	7.4 ± 11.6	
sAHP AMP (mV)	6.0 ± 8.2	12.0 ± 4.7	
sADP AMP (mV)	−6.2 ± 5.5	0.0 ± 0.0	

Values of variables resulting from division of cells into singlet and doublet groups. Singlet cells had a single action potential as a first observed suprathreshold event or a first interspike interval greater than 7 ms. Doublet cells fired more than one action potential as their first observed suprathreshold event and had a first interspike interval less than 7 ms. Cells in this table were screened by outlier selection criteria, resulting in a sample size of 70. The two groups thus formed were tested for significant differences using one-way ANOVAs. Variables that were significantly different are indicated by asterisks (* $P < 0.05$, ** $P < 0.01$).

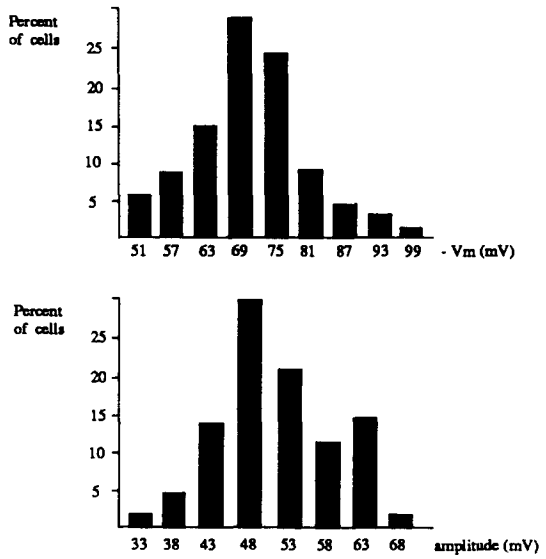

Fig. 2. Examples of smooth and 'notched' distributions (for explanation of bin size selection, see text). Top: the distribution of V_m for all cells in this sample. This distribution appears unimodal, and is similar to that for 25 of the 29 variables examined. Bottom: the distribution of action potential amplitudes for all cells in this sample. Its 'notched' appearance suggests that it may be composed of two distributions. To examine this possibility, a division was made into two groups at 57.5 mV, and these were analyzed for significant differences. Only 4 of the 29 variables examined showed 'notched' distributions.

Four of the distributions (INT2, TAU, AMP, and SAG), however, showed a 'notch' which separated the distribution into two peaks and suggested that it might be bimodal. In addition, five categorical variables (e.g. presence or absence of a fast after-hyperpolarization (fAHP) or a slow after-depolarization (sADP)) were also measured for each cell, and these by definition divided the data set into categories.

Among the cells that simultaneously satisfied both sets of selection criteria, two types of divisions were tried: continuous and categorical. Continuous divisions were made among the four distributions noted above which showed notches. Cells that corresponded to values of the variable which were above the notch were put into one group, while those that were below the notch were put into another (see Fig. 2 for example). After the division was made, a one-way ANOVA was performed on each of the remaining variables to test for significant group differences. The results of these divisions are summarized in Table 2. The greatest number of significant differences (10) was created by the AMP division, while the fewest was created by the SAG division (0). It is interesting to note that an arbitrary division in the distribution of INT1, which did not display a notch, also produced significant differences in four variables.

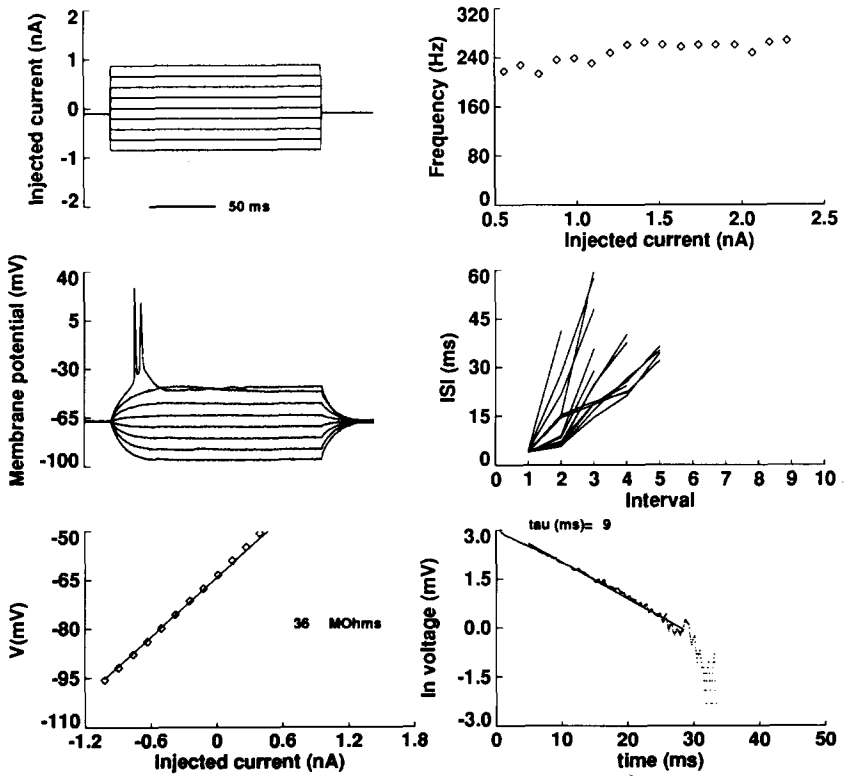

Fig. 3. Doublet cell characteristics. Left column: (upper) plot of injected current; (middle) corresponding voltage traces (some sweeps omitted for clarity); (lower) current–voltage relationship with input resistance. Right column: (upper) frequency of first interspike interval as a function of injected current (note how frequency of initial doublet remains relatively constant); (middle) interspike interval as a function of interval number (note how first intervals are all of similar length); (lower) natural logarithm of membrane potential plotted as a function of time with time constant.

The divisions made with respect to the five categorical variables (APP, fAHP, fADP, sAHP, sADP) were tested in the same way. The greatest number of significant differences was 8, and occurred between the cells that had a slow after-hyperpolarization (sAHP = 1) and those that did not (sAHP = 0). Only one significant difference was created by the divisions with respect to fast after-hyperpolarization (fAHP) and fast after-depolarization (fADP). These results are summarized in Table 3.

One 'composite' division was also tried in which cells were selected on the basis of one categorical (APP) and one continuous variable (INT1). Cells that fired an action potential pair as their first observed suprathreshold event (APP = 1) and had a first interspike interval less than seven milliseconds (INT1 < 7 ms) were grouped together. These criteria are similar to those used by other researchers [4,17] to identify intrinsically bursting cells. When this division was made, seven variables were significantly different between classes. This division was also made separately on the cells screened by the standard and outlier selection methods, and in each case it produced seven significant differences in the DU cells. When applied to the DF cells, however, no significant differences were found. These results are summarized in Table 4.

3.4. Cell characteristics

It should be clear from the previous section that there were several ways of dividing the cells into different groups. Although many of these ways produced a nearly equal number of significant differences, it is beyond the scope of this paper to discuss the characteristics of the cell classes formed by each of these divisions. Of all the divisions made, only the composite division corresponded to the classification scheme of RS and IB cells discussed in the literature. Because this scheme was consistent with previous work [4,17], and was not markedly inferior to the other schemes tried, it was chosen as the framework for describing cell characteristics in this paper. In addition, since the results obtained by the standard and outlier selection criteria were essentially the same for DU cells with the composite division, only the results obtained using the outlier selection criteria will be discussed below for the sake of clarity.

3.5. Doublet cells

Doublet cells were classified as those cells which fired at least two action potentials as their first observed suprathreshold event and which had a first

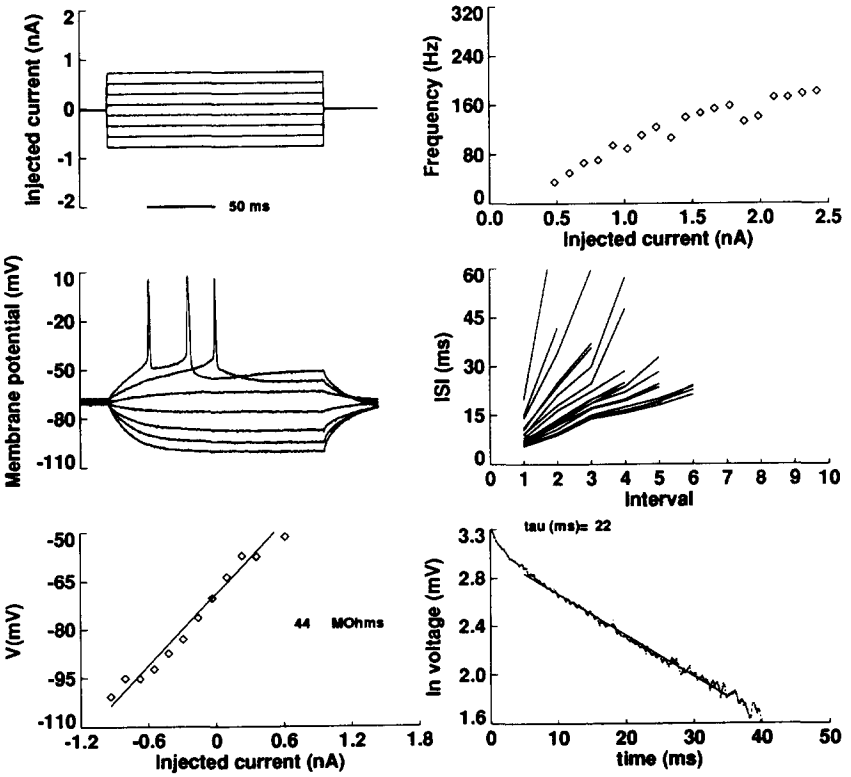

Fig. 4. Singlet cell characteristics. Left column: (upper) plot of injected current; (middle) corresponding voltage traces; (lower) current–voltage relationship with input resistance. Right column: (upper) frequency of first interspike interval as a function of injected current (note how frequency increases with current, in contrast to doublet cells); (middle) interspike interval as a function of interval number (note how first intervals have a variety of lengths); (lower) natural logarithm of membrane potential plotted as a function of time with time constant.

interspike interval of less than 7 ms (Fig. 3). About 20% (14/70 : DU, 6/10 : DF) of the cells in this sample were found to satisfy these criteria, and although all layers of perirhinal cortex were sampled, somata of these cells were found only in the middle layers (III–V). As mentioned before, the selection criteria used here were chosen to screen for cells that were similar to those described by other studies as intrinsically bursting (IB). In the literature, IB cells are reported to have several distinguishing characteristics: at least three action potentials are fired on the crest of a depolarizing wave; the burst is activated in an all-or-none manner; hyperpolarization can block the bursting mechanism [4,17]. The doublet cells in this study rarely fired more than two action potentials, and often did not show a pronounced depolarizing wave. In fact, only three cells encountered in this study had stereotypical bursting responses and could be considered IB cells by the criteria described above. The passive membrane properties of doublet cells (RIN, VM, TAU, SAG, UNDERSHOOT), were not significantly different from those of other cells, but it is worth noting that the cells which showed the largest amounts of sag were consistently members of the doublet class.

The action potentials fired by doublet cells usually had a characteristic sequence. The first action potential was narrow and was always followed by a fast after-hyperpolarization (fAHP), then by a second action potential of longer duration, which was usually

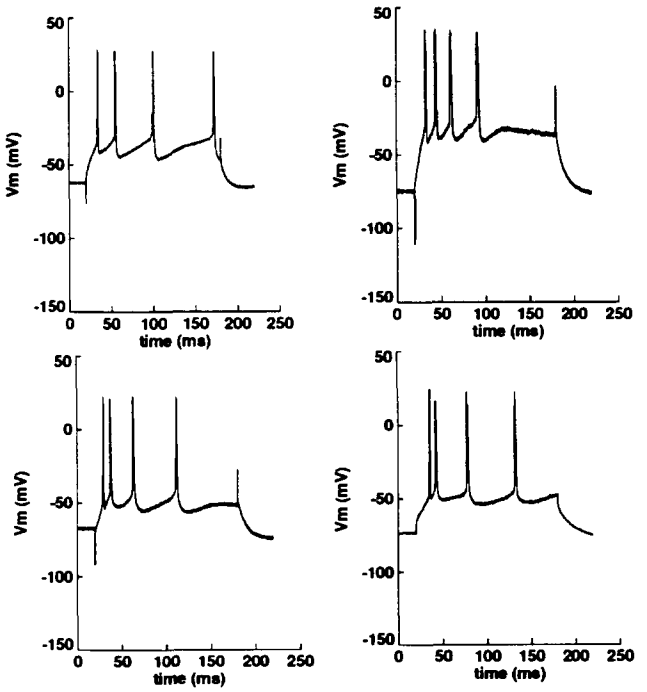

Fig. 5. Varieties of accommodation in different singlet cells. Interspike intervals could increase by a constant amount every interval (upper left and upper right), or could increase by a non-constant amount every interval (lower left and lower right).

(10/14, 71%) followed by a slow after-hyperpolarization (sAHP). Doublet cells had significantly larger amplitudes, (55.6 ± 5.8 mV, $P < 0.05$), smaller action potential widths at half-amplitude (1.0 ± 0.2 ms, $P < 0.05$), greater rates of rise (47.6 ± 8.5 V/s, $P < 0.01$) than other cells. In addition, the latencies of their fAHPs were significantly shorter (2.4 ± 0.8 ms, $P < 0.05$) and the sizes of their fAHPs were significantly greater (10.3 ± 6.1 mV, $P < 0.01$) than those of other cells.

With respect to repetitive firing, doublet cells had a lower mean rate of accommodation (3.1 ± 3.2 ms/interval), but this difference was not significant. Increases in spike frequency as a function of injected current (fI slope) were also lower, but not significantly different from other cells.

3.6. Singlet cells

Singlet cells were defined as all those cells which fired only one action potential as their first observed suprathreshold event or which had a first interspike interval greater than 7 ms (Fig. 4). About 80% (56/70 : DU, 4/10 : DF) of the cells in this sample were of this class, and their somata were found in all cortical layers (I–VI). These selection criteria were chosen so that cells identified as RS cells by other studies would be members of the singlet class.

Singlet cells were not significantly different from doublet cells in any of their passive membrane properties.

The action potentials fired by singlet cells were diverse and displayed a wide variety of afterpotentials. Of those singlet cells that did show fAHPs (46/56, 82%), their latencies were significantly longer (9.8 ± 23.3 ms, $P < 0.05$), and their magnitudes were significantly less (1.9 ± 8.6 mV, $P < 0.01$) than those of doublet cells. Half of the singlet cells in this sample (28/56, 50%) showed a fast after-depolarization (fADP) which followed the fAHP. Slow after-hyperpolarizations (sAHPs) were also present (31/56, 55%), and slow after-depolarizations (sADPs) occurred in a few cells (4/56, 7%), in contrast to doublet cells, where they were never seen. Singlet cells also fired action potentials with significantly smaller amplitude (49.5 ± 9.1 mV, $P < 0.05$), larger width at half-amplitude (1.3 ± 0.3 ms, $P < 0.05$) and lower rates of rise (39.3 ± 10.57 V/s, $P < 0.01$).

The repetitive firing behavior of singlet cells was not significantly different from that of doublet cells, perhaps because singlet cells displayed such a diversity of spiking sequences. In general, singlet cells showed spike-frequency accommodation, but this was present in differing degrees. Some cells showed gradual accommodation, while others fired two action potentials closely together before displaying accommodation (Fig. 5).

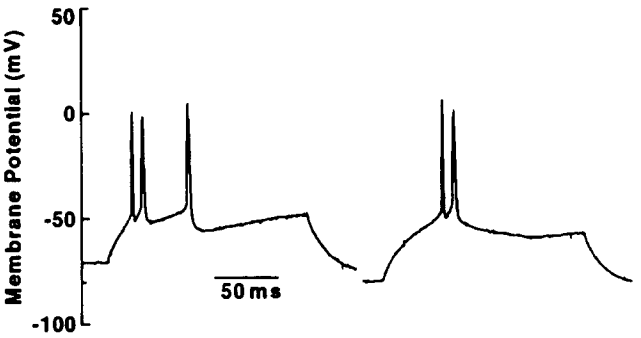

Fig. 6. Effects of injecting hyperpolarizing current on spiking patterns in a doublet cell. Left: cell response at resting membrane potential (−71 mV) to current step of +0.4 nA. Right: response of same cell to same current step when first hyperpolarized (−80 mV) by injection of −0.3 nA holding current. Hyperpolarization does not clearly transform this cell from transfer mode to bursting mode, since in both cases it fired a spike doublet. All doublet cells examined failed to show clear transition to bursting mode upon hyperpolarization.

3.7. Fast-spiking cells

In addition to doublet and singlet cells, cells similar to FS cells as described in the literature [4,17,26] were infrequently encountered (2/93 impalements). Because it was difficult to maintain stable recordings for more than five min in these cells, data on them were insufficient to establish a separate cell class for comparison in this study. Nevertheless, Fig. 10 shows results from one such recording. These cells had many of the features that are reportedly characteristic of FS cells: narrow spike width, a pronounced fAHP, and relatively little spike-frequency accommodation [17].

3.8. Hyperpolarizing and depolarizing manipulations

It has been shown in other studies that the spiking patterns of IB cells can be modulated by changes in resting membrane potential [4,16,17,21]. When depolarized, these cells enter a 'transfer' mode where they fire action potentials at a nearly constant rate and the frequency of firing is roughly proportional to the amount of depolarizing current injected. When hyperpolarized, though, IB cells fire in burst mode as previously described. To see if similar results could be obtained in this study, over 20 cells were given the current–voltage protocol (described in methods) while either hyperpolarized or depolarized from rest in cur-

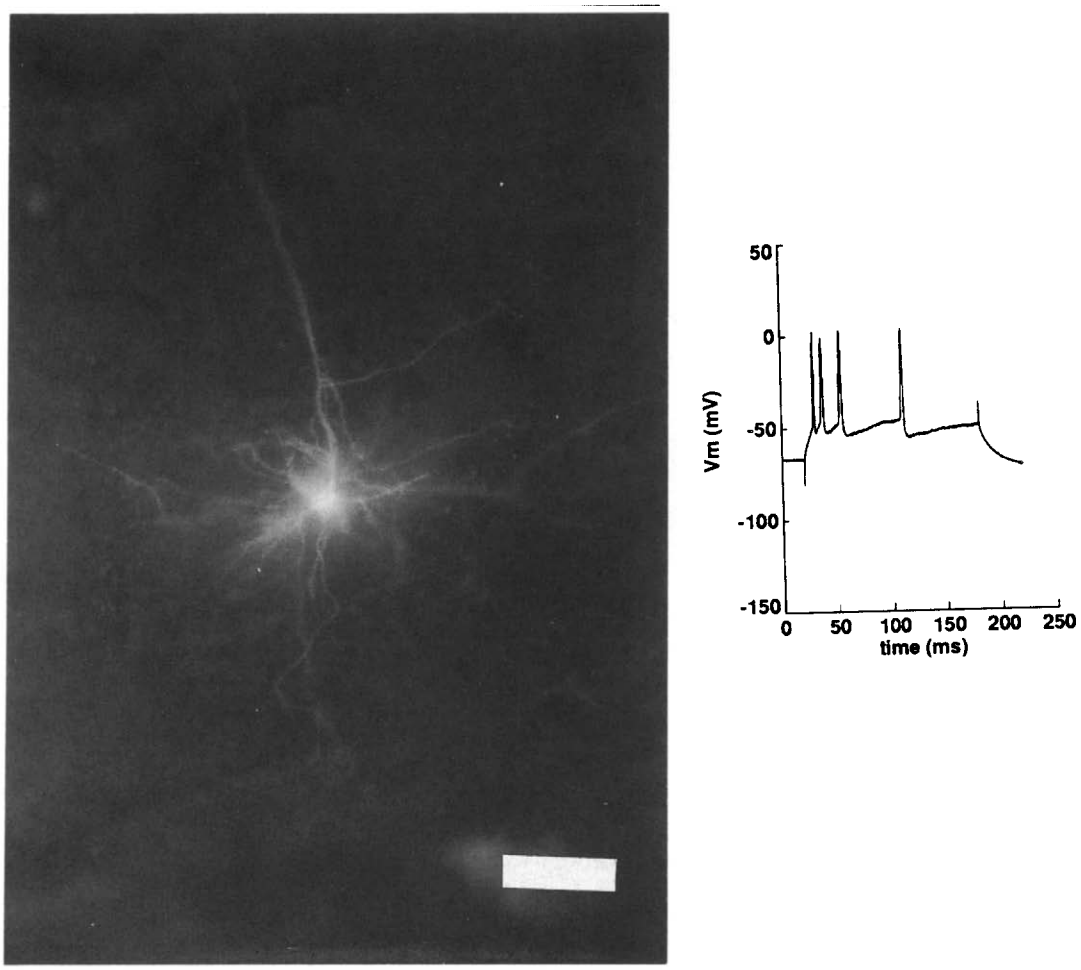

Fig. 7. Morphology of 'thin' cell, with accompanying membrane response to injected current step. Scale bar = 100 μM.

rent-clamp. In all cases the effects of these manipulations did not substantially change the firing mode of the singlet or doublet cells (Fig. 6).

3.9. Morphology

Although most recordings in this study were done without carboxyfluorescein, the presence of this dye in a few of the electrodes (14/93, 14%) allowed morphological information to be gathered from some of the cells. Because this dye is fluorescent and fades within a few days, the injected cells were best viewed within a few hours after filling, thus preventing detailed serial reconstructions. The morphological information presented here therefore only represents what could be viewed near one focal plane.

Two general morphologies were seen. The 'thin' type (Fig. 7) had a soma that was rounded with a single, sparsely branched apical dendrite oriented toward the pia. The basal dendrites of this type were numerous, and extended almost equally in all directions from the soma. The diameter of the apical and basal dendrites were roughly the same in the 'thin' type cells. In many respects, this type resembled the 'L 2/3' and 'slender L5' cells seen by Larkman and Mason [15,16] in rat visual cortex. Recordings from 11 of these cells were diverse, with 9 falling into the category of singlet cells, while the remaining 2 were doublet cells.

In contrast, the 'thick' type (Fig. 8) had a soma that was mote pyramidally shaped, with a longer, more extensively branched apical dendrite that was noticeably thicker than the basal dendrites, which were oriented laterally. This type was similar to the 'Thick L5' cells seen by Larkman and Mason [15,16]. The two 'thick' cells filled had electrophysiological properties of doublet cells.

One neuron was filled that was morphologically intermediate between these two types, having a pyramidal soma and a short but relatively thick apical

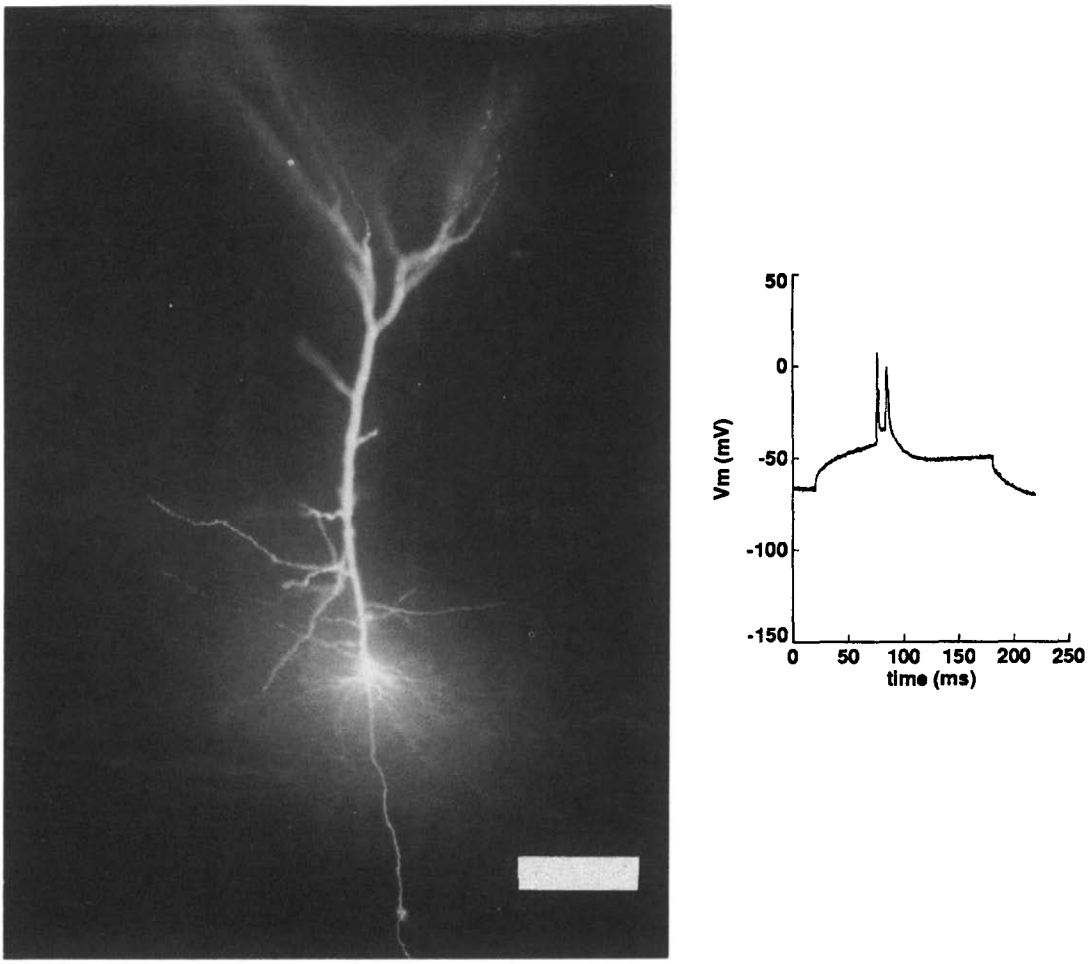

Fig. 8. Morphology of 'thick' cell, with accompanying membrane response to injected current step. Cell is located directly beneath the rhinal sulcus, and apical dendrites enter superficial layers of both dorsal and ventral banks of the sulcus. Scale bar = 100 μM.

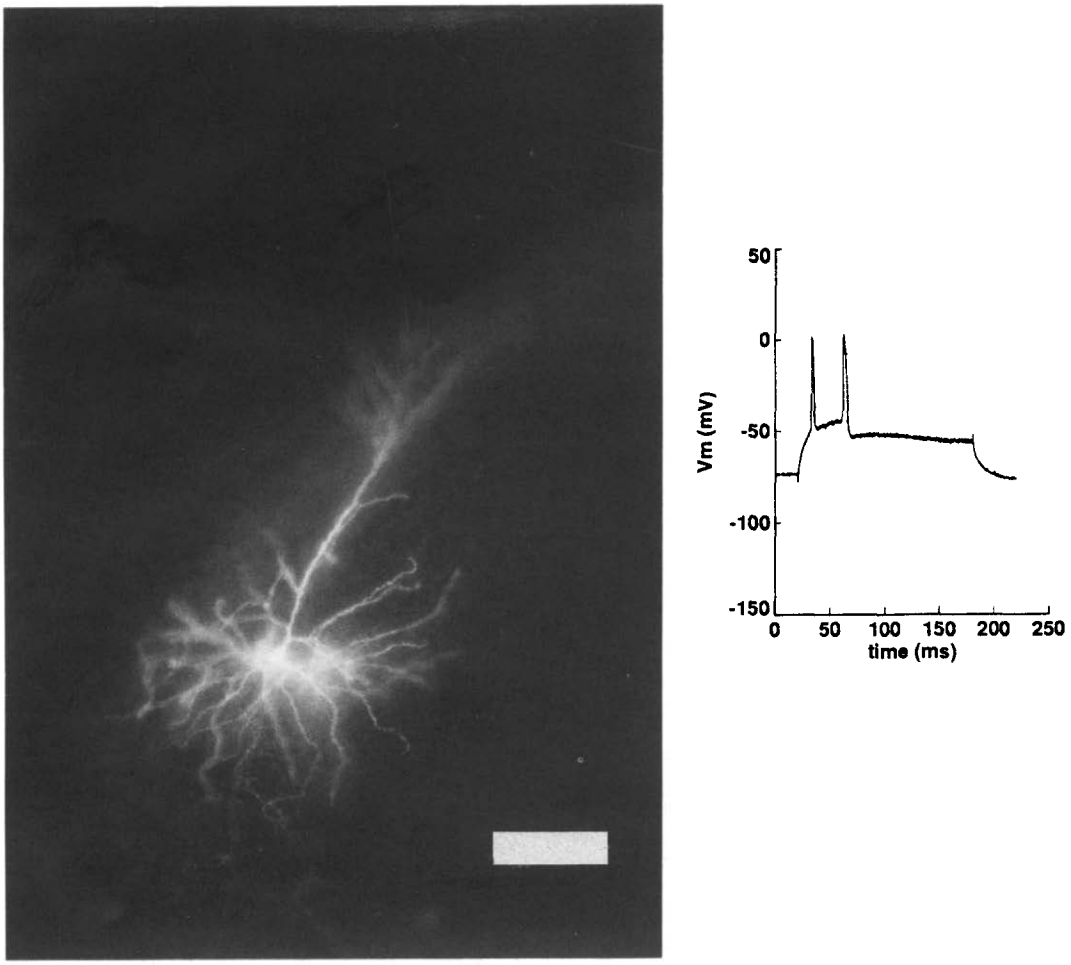

Fig. 9. Morphology of intermediate cell, with accompanying membrane response to injected current step. Scale bar = 100 μM.

dendrite (Fig. 9). Electrophysiologically, this cell was classified as a singlet cell.

4. Discussion

4.1. Main findings

This study of neurons in perirhinal cortex produced three main findings. (1) Under the 'standard' (but not 'outlier') selection criteria, cells recorded with carboxyfluorescein filled electrodes had significantly greater action potential widths at half-amplitude and more depolarized resting potentials than cells recorded without this dye. (2) A classification scheme similar to that used in other cortical studies produced cell classes with significant differences in seven variables. Several other schemes produced a greater number of differences, however, demonstrating that the choice of the best classification scheme is not obvious. (3) The cells encountered displayed a diversity of electrophysiological properties, and were similar with regard to spiking patterns, afterpotentials, and morphology to cells reported in other cortical areas. (4) Relatively few (4%) IB cells were encountered in perirhinal cortex.

4.2. Dye effects

Although the sample size of DF cells was small ($N = 14$), they were significantly different from the DU cells when both groups were selected by the 'standard' criteria. In contrast, under 'outlier' selection criteria there were no significant differences. The fact that action potential width at half-amplitude was broader and resting membrane potential was more depolarized in DF cells selected by 'outlier' criteria raises the possibility that carboxyfluorescein contributed to these changes. It is also interesting to note that among the DF cells, no significant differences were found between the doublet and singlet cells. This may be because electrophysiological properties of doublet and singlet cells moved toward a common point, causing the two types to become statistically indistinguishable. Rao and colleagues [27] also used carboxyfluorescein and reported that action potential amplitudes decreased during the course of dye filling, although they

mentioned that no similar decrease was seen in resting membrane potential. While this study was not designed expressly to probe the effects of carboxyfluorescein, these results along with those of Rao and coworkers should be sufficient to show that this dye can alter electrophysiological properties when used in intracellular electrodes. While biocytin has been shown to cause no significant changes in electrophysiological properties [34], it requires more complicated processing steps than carboxyfluorescein.

4.3. Classification schemes

For the sake of comparison with previous classifications reported in the literature, the cells in this study were described within the framework of singlet and doublet cells. This scheme was designed to be similar to that of RS and IB cells, a scheme which has guided work over several years [1,4,5,15,16,17]. It is unclear, though, whether this is the only scheme that can be used successfully to classify cortical neurons. It is also unclear what the best strategy would be to arrive at an optimal classification.

Cell classifications are used for a variety of purposes. Physiologists recording from slices can use knowledge about spiking patterns to infer whether the synaptic effects of a cell will be inhibitory or excitatory; physiologists recording from behaving animals can match spiking patterns with connectivity of certain cell types to infer the activity of a projecting brain region; modelers can use anatomical information about morphology and connectivity to imbue a network of cells with their appropriate spiking patterns; in the future, histochemical labeling of channel densities may be combined with morphology to construct models with appropriate spiking output. In all of these cases, information about one characteristic is used to make inferences about other characteristics. The development of a cell classification scheme should therefore reflect this need.

As described in the results section, a classification was sought that would support inferences about cell properties. Thus, the classification that would allow the greatest number of independent inferences to be made was judged to be the best. These inferences could be made most easily when the properties of one class of neuron were significantly different from the properties of another class, and when the properties of a given class all covaried together.

To approach the issue of classification systematically was not the goal of this study. Rather, alternative classification schemes were sought merely to explore whether it was possible to group the cells with reasonable success without using the established scheme (RS, IB, and FS). Using the number of statistically significant differences between groups as a crude measure of success, the results suggest that other schemes might also be used to effectively classify the cells of this data set.

It is not known whether data from other cortical regions could also support alternative classifications, or whether the results obtained in this study merely reflect the population of cells found in perirhinal cortex. Foehring and coworkers [9] did not find any intrinsically bursting cells in their survey of human association cortex, but they did encounter 'low-threshold spiking' cells (LTS cells) that appeared to be similar to some of the doublet cells found in this study. Because the cells that they found did not fit into the established scheme, their data might also be amenable to the alternative groupings used on perirhinal cells. In regions where IB cells are clearly present, alternative groupings may not be successful, but this has not been tried.

The proper approach to classifying cortical cells would be accomplished best through more sophisticated techniques involving cluster analysis [20]. This is currently being considered as an approach to be used on this data set, but awaits further investigation. Questions of interest that might be answered by this approach might include: How many natural groups are there? How many different ways can the data set be successfully divided?

4.4. Cell types

Despite the fact that the cells encountered in this study did not support the established scheme of RS, IB, and FS cells as the only natural grouping, a number of cells did appear to be strikingly similar to the RS and IB cells reported by others. Prototypical RS and IB cells can be seen in Fig. 10, but these were encountered infrequently. More often, cells appeared to have characteristics intermediate to these two examples. Prototypical FS cells were impaled rarely (Fig. 10). It is likely that inhibitory neurons with fast-spiking properties are abundant in perirhinal cortex, as anatomical studies suggest [13], but that microelectrode recording is not an accurate way of estimating their numbers.

4.5. Relative scarcity of IB cells

Only three cells encountered in this study had stereotypical bursting responses, where three to five action potentials were fired in quick succession on the crest of a depolarizing wave. The remainder of the doublet cells fired no more than two action potentials closely together as their first observed suprathreshold event, and rarely showed a depolarizing envelope. Even when hyperpolarized, doublet cells failed to show complexes of multiple spikes that are characteristic of bursting cells. Does this indicate a relative lack of IB cells in perirhinal cortex? It would be difficult to

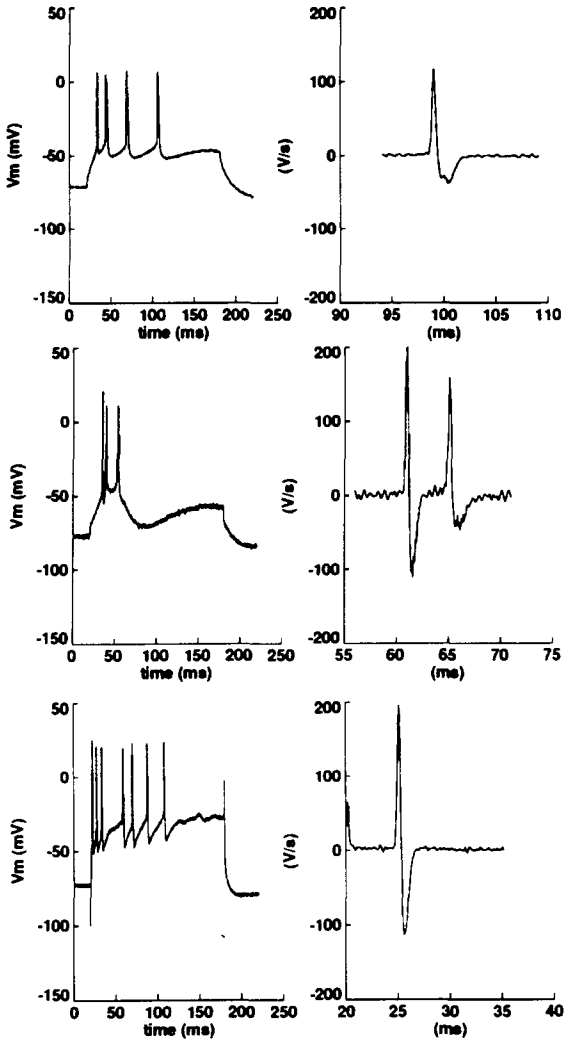

Fig. 10. Spiking patterns and derivatives of action potentials for a singlet cell, a bursting cell, and a fast-spiking cell in response to injected depolarizing current step. Top: singlet cell shows spike-frequency accommodation. Derivative shows that magnitude of spike upstroke (V/s) is more than twice the magnitude of downstroke. Also, upstroke duration is approximately one-third of downstroke duration. Middle: bursting cell has three action potentials fired on top of a depolarizing envelope, followed by an AHP of over 50ms. Derivatives for bursting cell show that for the first action potential, magnitude of upstroke (V/s) is less than twice that of downstroke, and downstroke duration is approximately twice that of upstroke. Derivative of the second action potential is smaller in magnitude, and in proportions is similar to the action potential of singlet cell. Bottom: fast-spiking cell shows high-frequency firing and little accommodation. Derivative of fast-spiking cell is similar in magnitude and proportions to derivative of first action potential of bursting cell.

conclude this from the recordings made in this study alone, since there may have been a particular electrode bias that prevented IB cells from being impaled and/or maintained. The fact that Foehring and coworkers [9] did not find any IB cells in human association cortex is suggestive of a scarcity, however. It will be interesting to see if a similar paucity of IB cells will be seen by other workers or in other brain regions. The roles that IB cells may play in a cortical circuit are still being investigated [30], but their presence or absence in certain brain regions may give some clues to their functions.

Some remarks about the protocols for identifying cells are now in order. While the amount of injected current was not manually controlled, it was injected in increments of 0.1 nA. This may not have always been precise enough to determine whether the first suprathreshold event would have been a single spike or a doublet complex. One possible objection to this method is that it may have led to misclassified cells. There are several reasons why this is unlikely to have been a problem. Inspection of the recordings reveals that although there were some cases of cells which fired single action potentials as their first suprathreshold event and then later consistently fired doublets, this happened only five times (5/70, 7%). Thus only a small number of doublet cells might have been misclassified as singlet cells. If a conservative estimate of the misclassification rate is 7%, then it is unlikely that more than one of the 14 doublet cells sampled would have actually fired a single action potential if the current steps had been applied in smaller increments. So it is probable that even fewer singlet cells were misclassified as a doublet cells.

The action potentials recorded for both singlet and doublet cells in this study were somewhat slower, wider, and shorter than those recorded by others in studies of cortical pyramidal neurons [16,17]. This point deserves to be addressed, since it raises the possibility that the impalements were poor, or that the recording apparatus was configured with a narrow bandwidth. Neither of these are likely possibilities, however. By all other measures, the impalements in this study were good, given that the average values for membrane potential (VM) and input resistance (RIN) were well within the range of those given in the other studies where action potentials were reported to be narrower and larger. Also, poor impalements should preclude long recording times, yet the duration of the impalements in this study were typically 30 min or more, sometimes lasting several hours. It is also unlikely that the bandwidth was too narrow, given that some of the cells recorded had action potentials with rising slopes (349 V/s), widths (0.65 ms), and amplitudes (68 mV) commensurate with those found in other studies. This demonstrates that the recording apparatus was able to record such action potentials when they occurred. Apparently, the values reported here for action potentials are reflective of cells in perirhinal cortex and are not artifactual.

Concerning this point, it should also be mentioned that the bathing fluid used in this study was composed

of 2 mEq [K^+], as opposed to 5–6 mEq [K^+], which has been used in other studies of neocortical classification [4,17]. While this lower value of [K^+] may account for some differences in spike width and slope, it mimics the range of K^+ found in the extracellular fluid of the brain. The use of unphysiologically high levels of K^+ has long been questioned as unnecessary [8], and may contribute to increased neuronal excitability [23].

Is there a common mechanism that could be used to explain the differences between singlet and doublet cells? It has been suggested that a transient calcium current (I_t) that is activated at voltages below −65 mV is responsible for the depolarizing envelope in bursting cells [10]. Because the doublet cells in this study did not show marked differences in their firing patterns upon hyperpolarization, it is unlikely that such a current exists in them. Montoro and coworkers [21] have shown that some neocortical neurons have a burst mechanism that is inactivated by TTX. This sodium conductance is not activated by hyperpolarization and might be responsible for doublet firing, but this cannot account for many of the other significant differences that were found between the doublet and singlet classes. Rather, the primary feature that distinguishes doublet cells is their rapid and strong after-hyperpolarization. This can account for significantly shorter fAHP latency, greater fAHP magnitude, shorter action potential width, greater maximum fall rate, and shorter first interspike interval. It could be supposed that these effects are caused by a fast potassium repolarization current like I_c, which is known to contribute to fAHPs in neocortical neurons [29]. This is not likely though, since Schwindt and coworkers [29] found that bursting increased when this conductance was blocked, an effect apparently caused by inadequate spike repolarization. An answer to the mechanism underlying doublet generation will have to await pharmacological analysis.

Conclusions about the morphologies of these cell classes should not be drawn firmly, since the sample size of DF cells was relatively small. It is interesting, though, that both of the filled cells with 'thick' morphologies were doublet cells. This is in agreement with the findings of other researchers [3,15,16], who have suggested that IB cells have larger and thicker apical dendrites than RS cells. The fact that cells with 'thin' morphologies had diverse electrophysiological properties would suggest that it is not possible to infer cell structure from electrophysiological recording alone. In addition, the presence of a cell with intermediate morphology indicates that the diversity of cells within perirhinal cortex is far greater than can be portrayed by this study. Perhaps a more detailed classification scheme could encompass this diversity and allow more subtle inferences to be made between structure and morphology, but such a scheme has yet to be developed.

4.6. Future directions

The first step toward understanding the functions of a cortical circuit must begin with an understanding of its constituents. Hopefully, the results of this study will provide a basis for future explorations of perirhinal cortex, an area currently receiving much research attention. As mentioned in section 1, perirhinal cortex has been implicated in mnemonic function in the rat [2,28]. Specifically, lesions of perirhinal cortex block the expression of fear-potentiated startle [28].It is also known that perirhinal cortex has extensive reciprocal connections with the amygdala [18,24], another structure necessary for acquisition of startle behavior [6]. It will be of particular interest to determine which cell classes send or receive amygdaloid projections, and which cell classes can support use-dependent synaptic plasticity. In this way, progress might be made toward understanding how cortical circuits might contribute to the formation and storage of memories.

Acknowledgements

This work was supported by NIH and Yale University. We would also like to thank the two anonymous reviewers who provided critical comments for improving this manuscript.

References

[1] Agmon, A. and Connors, B.W., Correlation between intrinsic firing patterns and thalamocortical synaptic responses of neurons in mouse barrel cortex, *J. Neurosci.*, 12 (1992) 319–329.

[2] Campeau, S., *Behavioral and neural analysis of the central auditory pathways involved in fear conditioning as measured with the fear-potentiated startle paradigm using auditory conditioned stimuli*, Yale University thesis, 1993.

[3] Chagnac-Amitai, Y., Luhmann, H.J. and Prince, D.A., Burst generating and regular spiking layer 5 pyramidal neurons of rat neocortex have different morphological features, *J. Comp. Neurol.*, 296 (1990) 598–613.

[4] Connors, B.W., Gutnick, M.J. and Prince, D.A., Electrophysiological properties of neocortical neurons in vitro, *J. Neurophysiol.*, 48 (1982) 1302–1320.

[5] Connors, B.W. and Gutnick, M.J., Intrinsic firing patterns of diverse neocortical neurons, *Trends Neurosci.*, 13 (1990) 99–104.

[6] Davis, M., The role of the amygdala in fear and anxiety, *Annu. Rev. Neurosci.*, (1992) 353–375.

[7] Deacon, T.W., Eichenbaum, H., Rosenberg, P. and Eckman, K.W., Afferent connections of the perirhinal cortex of the rat, *J. Comp. Neurol.*, 220 (1983) 168–190.

[8] Dingledine, R.D., Dodd, J. and Kelly, J.S., The in vitro brain slice as a useful neurophysiological preparation for intracellular recording, *J. Neurosci. Methods*, 2 (1980) 323–362.

[9] Foehring, R.C., Lorenzon, N.M., Herron, P. and Wilson, C.J., Correlation of physiologically and morphologically identified neuronal types in human association cortex in vitro, *J. Neurophysiol.*, 66 (1991) 1825–1837.

[10] Friedman, A. and Gutnick, M.J., Low-threshold calcium electrogenesis in neocortical neurons, *Neurosci. Lett.*, 81 (1987) 117–122.

[11] Grace, A.A. and Llinas, R., Electrophysiology and morphology of four classes of prefrontal neocortical neurons studied in vitro, *Soc. Neurosci. Abstr.*, 10 (1984) 302–320.

[12] Kairiss, E.W. and Beggs, J.M., Synaptic physiology of neurons in rat perirhinal cortex, *Soc. Neurosci. Abstr.*, 19 (1993) 1445.

[13] Kosel, C.K., *The anatomical organization of the parahippocampal corticies in the rat*, Universtiy of Iowa thesis, 1981.

[14] Keller, A., Iriki, A. and Asanuma, H., Identification of neurons producing long-term potentiation in the cat motor cortex: intracellular recordings and labeling, *J. Comp. Neurol.*, 300 (1990) 47–60.

[15] Larkman, A. and Mason, A., Correlations between morphology and electrophysiology of pyramidal neurons in slices of rat visual cortex. I. Establishment of cell classes, *J. Neurosci.*, 10 (1990) 1407–1414.

[16] Mason, A. and Larkman, A., Correlations between morphology and electrophysiology of pyramidal neurons in slices of rat visual cortex. II. Electrophysiology, *J. Neurosci.*, 10 (5), (1990), 1415–1428.

[17] McCormick, D.A., Connors, B.W., Lighthall, J.W. and Prince, D.A., Comparative electrophysiology of pyramidal and sparsely spiny stellate neurons of the neocortex, *J. Neurophysiol.*, 54 (4) (1985) 782–806.

[18] McDonald, A.J. and Jackson, T.R., Amygdaloid connections with posterior insular and temporal cortical areas in the rat, *J. Comp. Neurol.*, 262 (1987) 59–77.

[19] Meunier, M., Bachevalier, J., Mishkin, M. and Murray, E.A., Effects on visual recognition of combined and separate ablations of the entorhinal and perirhinal cortex in rhesus monkeys, *J. Neuroscience*, 13 (1993) 5418–5432.

[20] Milligan, G.W., A review of monte-carlo tests of cluster analysis, *Multivariate Behav. Res.*, 16 (1981) 379–407.

[21] Montoro, R.J., Lopez-Barneo, J., Jassik-Gerschenfeld, D., Differential burst firing modes in neurons of the mammalian visual cortex in vitro, *Brain Res.*, 460 (1988) 168–172.

[22] Murray, E.A. and Mishkin, M., Visual recognition in monkeys following rhinal cortical ablations combined with either amygdalectomy or hippocampectomy, *J. Neurosci.*, 6 (1986) 1991–2003.

[23] Ogata, N., Hori, N. and Katauda, N., The correlation between extracellular potassium concentration and hippocampal epileptic activity in vitro, *Brain Res.*, 110 (1976) 371–375.

[24] Otterson, O. Connections of the amygdala of the rat. IV. Corticoamygdaloid and intra-amygdala connections as studied with axonal transport of horseradish peroxidase, *J. Comp. Neurol.*, 205 (1982) 30–48.

[25] Paxinos, G. and Watson, C., *The Rat Brain in Stereotaxic Coordinates*, San Diego, Academic Press, 1986.

[26] Pockberger, H., Electrophysiological and morphological properties of rat motor cortex in vitro, *Brain Res.*, 539 (1991) 181–190.

[27] Rao, G., Barnes, C.A. and McNaughton, B.L., Intracellular flourescent staining with carboxyfluorescein: a rapid and reliable method for quantifying dye-coupling in mammalian central nervous system, *J. Neurosci. Methods*, 16 (1986) 251–263.

[28] Rosen, J.B., Hitchcock, J.M., Miserendino, M.J.D., Falls, W.A., Campeau, S. and Davis, M., Lesions of the perirhinal cortex but not the frontal, medial, visual, or insular cortex block fear-potentiated startle using a visual conditioned stimulus, *J. Neurosci.*, 12 (1992) 4624–4633.

[29] Schwindt, P.C., Spain, W.J., Foehring, R.C., Stafstrom, C.E., Chubb, M.C. and Crill, W.E., Multiple potassium conductances and their functions in neurons from cat sensorimotor cortex in vitro, *J. Neurophysiol.*, 59 (1988) 424–449.

[30] Silva, L.R., Amitai, Y. and Connors, B.W., Intrinsic oscillations of neocortex generated by layer 5 pyramidal neurons, *Science*, 251 (1991) 432–435.

[31] Stafstrom, C.E., Scwindt, Flatman, J.A. and Crill, W.E., Properties of subthreshold response and action potential recorded in layer V neurons from cat sensorimotor neurons in vitro, *J. Neurophysiol.*, 53 (1984) 244–263.

[32] Squire, L.R. and Zola-Morgan, S., The medial temporal lobe memory system, *Science*, 253 (1991) 1380–1386.

[33] Terrell, G.R. and Scott, D.W., Oversmoothed nonparametric density estimates, Journal of the American Statistical Association, 80 (1985) 243–249.

[34] Tseng, G., Parada, I. and Prince, D.A., Double-labelling with rhodamine beads and biocytin: a technique for studying corticospinal and other projection neurons in vitro, *J. Neurosci. Methods*, 37 (1991) 121–131.

[35] Tukey, J.W., *Exploratory Data Analysis*, Reading, Massachusetts, Addison Wesley, 1977.

[36] Zola-Morgan, S., Squire, L.R., Amaral, D.G. and Suzuki, W.A., Lesions of perirhinal and parahippocampal cortex that spare the amygdala and hippocampal formation produce severe memory impairment, *J. Neurosci.*, 9 (1989) 4355–4370.